VESSEL DENSITY OF SUPERFICIAL, INTERMEDIATE, AND DEEP CAPILLARY PLEXUSES USING OPTICAL COHERENCE TOMOGRAPHY ANGIOGRAPHY

CARLO LAVIA, MD,*† SOPHIE BONNIN, MD,* MILENA MAULE, PhD,‡ ALI ERGINAY, MD,* RAMIN TADAYONI, MD, PhD,* ALAIN GAUDRIC, MD*

Purpose: To provide values of retinal vessel density (VD) in the three retinal capillary plexuses, foveal avascular zone (FAZ) area, and retinal layer thickness in a cohort of healthy subjects.

Methods: The optical coherence tomography angiography maps of 148 eyes of 84 healthy subjects, aged 22 to 76 years, were analyzed for measuring VD of the retinal capillary plexuses, using the Optovue device comprising a projection artifact removal algorithm. Foveal avascular zone metrics were measured, and the relationship between optical coherence tomography angiography findings and age, sex, and image quality was studied.

Results: The deep capillary plexus showed the lowest VD (31.6% ± 4.4%) in all macular areas and age groups compared with the superficial vascular plexus (47.8% ± 2.8%) and intermediate capillary plexus (45.4% ± 4.2%). The mean VD decreased by 0.06%, 0.06%, and 0.08% per year, respectively, in the superficial vascular plexus, intermediate capillary plexus, and deep capillary plexus. Mean FAZ area, FAZ acircularity index, and capillary density in a 300-μm area around the FAZ were 0.25 ± 0.1 mm^2, 1.1 ± 0.05, and 50.8 ± 3.4%, respectively. The yearly increase in FAZ area was 0.003 mm^2 ($P < 0.001$).

Conclusion: The deep capillary plexus, a single monoplanar capillary plexus located in the outer plexiform layer, has the lowest VD, a significant finding that might be used to evaluate retinal vascular diseases. Vascular density decreased with age in the three capillary plexuses.

RETINA 39:247–258, 2019

Optical coherence tomography (OCT) angiography (OCTA) has allowed for the first time to distinguish different retinal capillary plexuses in vivo, which was not possible before with fluorescein angiography.[1,2] The presence of four capillary layers in the posterior pole has been well established histologically.[3–6] However, the first versions of OCTA software were only able to differentiate the superficial from the deep capillary layer within the macula and the peripapillary radial capillaries around the optic disk. When OCTA became available in clinical practice, it was used to quantify the severity of capillary nonperfusion in diabetic retinopathy, retinal vein occlusion, sickle cell disease, and in other conditions.[7–10] However, although retinal vessel density (VD) measurements were relatively accurate in the superficial vessel plexus, the assessment of the intermediate capillary plexus (ICP) and deep capillary plexus (DCP) was altered by projection artifacts originating from the superficial layers.[11]

The recent improvement in retinal segmentation and the development of algorithms removing projection artifacts (PAR)[12,13] have allowed for visualizing three capillary layers in the macula and measuring their respective densities.

The aim of this study was then to provide values of VD, foveal avascular zone (FAZ) area, and retinal layer thickness in a cohort of healthy subjects, using a commercially available OCTA device equipped with PAR algorithm, to provide a method for assessing the severity and evolution of retinal vascular diseases in the macula.

Subjects and Methods

Demographics

This study was conducted in a tertiary ophthalmology center (Lariboisière Hospital, Paris-Diderot University, Paris, France), was approved by the Ethics Committee

of the French Society of Ophthalmology (IRB 00008855 Societe Française d'Ophtalmologie IRB#1), and adhered to the tenets of the Declaration of Helsinki. Informed consent was obtained from all subjects.

A total of 91 healthy white subjects were enrolled to analyze the macular capillary VD in both eyes using OCTA.

To be included in the study, subjects had to meet the following criteria: presenting with no systemic disease, no media opacities, no history of eye surgery, retinal diseases or glaucoma in any eye, and having a refractive error ranging between -3 and $+2$ diopters. Subject age ranged between 22 and 76 years.

Optical Coherence Tomography Angiography Device

Optical coherence tomography angiography examination was performed with the RTVue XR Avanti (Optovue, Fremont, CA) spectral-domain OCT device with phase 7 AngioVue software. The OCTA device has a light source at 840 nm, a bandwidth of 45 nm, and an A-scan rate of 70.000 scans per second. Each scan

Reprint requests: Alain Gaudric, MD, Service d'Ophtalmologie, Hôpital Lariboisière, Assistance Publique-Hôpitaux de Paris, 2, rue Ambroise Paré, 75475 Cedex 10 Paris, France; e-mail; agaudric@gmail.com

consisted of 608 B-frames, composed of a set of 304 A-lines acquired 2 times at each of the 304 raster positions. The scanning area used in this study was 3 x 3 mm, centered on the fovea. To correct motion artifacts, OCTA combines orthogonal fast-scan directions (horizontal and vertical) and is equipped with the DualTrac Motion Correction technology. This technology uses a two-level approach: real-time correction for rapid eye movements or blinking and postprocessing correction of smaller motion distortions.[14]

The software includes the 3D PAR algorithm, which removes projection artifacts from the OCTA volume on a per voxel basis,[12,15] using information from the OCT and OCTA volume to differentiate in situ OCTA signal from projection artifacts.

Case Selection

Optical coherence tomography angiography scans from 182 eyes were then screened for image quality, and the signal strength index (SSI) and the quality index (QI) were assessed. In brief, although the SSI (range 1–100) reflects the signal strength, potentially confounded by age and eye diseases, the newer QI (range 1–10) accounts for signal strength and 2 adjunctive factors: motion artifacts and image sharpness. Images with SSI <70 and QI <7 were excluded. All scans were controlled by two experts for correctness of automated layer segmentation, as well as for FAZ delineation. In case of segmentation errors, manual corrections were performed by the examiners and then evaluated by a third expert. In case of segmentation errors involving more than 5% of the total scan area (i.e., 15 B-scans), the image was excluded from the analysis. Eyes with B-scan tilting exceeding 10° were also excluded. In total, 34 eyes were excluded from the analysis, of which 27 because of visible image artifacts (e.g., quilting/motion artifacts, 4 eyes; image tilting, 9 eyes; presence of segmentation errors or poor SSI/QI, 2 and 12 eyes, respectively). Seven other eyes were excluded because of the presence of a thin epiretinal membrane, lamellar macular hole (all discovered on the OCT B-scan), or image shadowing due to vitreous floaters.

Therefore, after the application of the OCTA inclusion and exclusion criteria, 148 eyes from 84 subjects (39 men and 45 women) were included in the analysis (Table 1). Subgroups were created based on the quintile distribution to be as uniform as possible with regard to age and sex.

Optical Coherence Tomography Angiography Analysis

Retinal blood flow was analyzed on both en face OCTA scans and B-scans, the former providing OCTA VD maps and VD data. Three vascular layers

Table 1. Demographic Data

	Overall	Male	Female
N subjects/eyes	84/148	39/67	45/81
Age: mean ± SD (range)	41.3 ± 15.9 (22.2–75.8)	42.0 ± 16.3 (23.4–75.8)	40.7 ± 15.7 (22.2–75.3)
Age quintiles: n subjects/eyes			
1: 22–26 y	17/34	9/18	8/16
2: 27–31 y	18/34	7/14	11/20
3: 32–39 y	13/24	6/11	7/13
4: 40–57 y	21/37	10/16	11/21
5: >58 y	15/19	7/8	8/11

were isolated and named according to the nomenclature proposed by Campbell et al.[15] In brief, from the inner retina toward the outer retina, we defined a superficial vascular plexus (SVP), an ICP, and a DCP. The ICP and the DCP were both parts of a deep vascular complex (DVC), which was also analyzed (Figure 1). The use of this nomenclature does not prejudge the functional flow pattern, which remains controversial. Some authors consider that the flow in the SVP, ICP, and DCP functions in parallel[15] while others suggest rather a serial organization of the blood flow.[4,16,17] Our data did not aim to solve this controversy.

We used the predefined boundaries provided by Optovue software for the SVP and the DVC analysis: the SVP was comprised between the inner limiting membrane (ILM) and 9 μm above the junction between the inner plexiform layer and the inner nuclear layer (IPL–INL), while the DVC was comprised between 9 μm above the IPL–INL junction and 9 μm below the outer plexiform layer and outer nuclear layer (OPL–ONL) junction; there was no overlap between the 2 slabs.

We then segmented the DVC into ICP and DCP by manually adjusting segmentation boundaries. The ICP boundaries were set between 9 μm above the IPL–INL junction and 6 μm below the INL–OPL junction, thus including parts of the IPL and OPL and all the INL to record the ICP projection that is located in the IPL.[5] The DCP boundaries were set between 6 μm below the INL–OPL junction and 9 μm below the OPL–ONL junction, thus including the OPL and showing the typical monoplanar lobular pattern of the DCP[3,4,16] (Figure 2).

Vessel Density Measurements

Automated VD was calculated using Phase 7 AngioAnalytic software in the SVP and the DVC, and VD of the customized ICP and DCP was analyzed using a research version of this software. In this software, the VD corresponds to the percentage of the surface occupied by vessels and capillaries based on adaptive thresholding binarization within the desired area. Vessel density and retinal thickness values were recorded for the whole 3 × 3-mm area, in the inner circle of the Early Treatment of Diabetic Retinopathy Study chart (i.e., the foveal area, 1-mm diameter circle) and in the parafoveal area (an annulus of 1.5-mm radius around the fovea) and its sectors (Figure 3). We also measured the FAZ area and perimeter and foveal acircularity index (i.e., the ratio between the measured perimeter and the perimeter of the same size circular area: a perfectly circular FAZ has an acircularity index equal to 1, with deviations from a circular shape leading to an increase in this metric). Foveal VD 300 (FD-300; i.e., VD in a 300-μm wide zone around the FAZ combining the SVP and the DVC), automatically calculated by the software, was also evaluated (Figure 3). Vessel density measurement in this area avoids to incorporate the FAZ, whose area is highly variable among individuals.[18] The values of FD-300 are complimentary to FAZ metrics and have been previously used to detect early signs of diabetic retinopathy.[19]

Retinal Layer Thickness Analysis

Retinal layer thickness was evaluated on the same 3 × 3-mm OCTA acquisitions as those used for the vessel analysis. The OCT software automatically segments retinal layers and provides retinal thickness values within 10 predefined slabs, from the ILM to the Bruch membrane, as shown in Figure 1. In this study, five slabs were selected for the analysis: one —ILM to retinal pigment epithelium (full retinal thickness: ILM–retinal pigment epithelium slab); two— ILM to IPL, including the thin optic nerve fiber layer (see **Figure 4, Supplemental Digital Content 1**, http://links.lww.com/IAE/A945) (ILM–IPL slab); three—NFL to IPL (ganglion cell layer [GCL]–IPL slab); four—IPL to OPL (INL–OPL slab); and five— IPL to ONL (INL slab).

Concordance Between Retinal Vessel Complexes and Retinal Layer Thickness

The concordance between VD in each vascular plexus and the thickness of the corresponding retinal

Fig. 1. Boundaries of retinal vascular plexuses and retinal layer segmentation. Optical coherence tomography B-scans with angio-flow showing the retinal segmentation in the different capillary plexuses (top and middle) and the segmentation of the retinal layers (bottom). **A.** B-scan showing the boundaries (red and green lines) that delineate the SVP between the ILM and 9 μm above the junction between the IPL–INL. **B.** B-scan showing the boundaries (green and red lines) that delineate the DVC between 9 μm above the IPL–INL junction and 9 μm below the OPL–ONL; there is no overlap between the 2 previous slabs. **C.** B-scan showing the boundaries (green and red lines) that delineate the ICP between 9 μm above the IPL–INL junction and 6 μm below the INL–OPL junction, thus including parts of the IPL and OPL and all the INL. **D.** B-scan showing the boundaries (red lines) that delineate the DCP between 6 μm below the INL–OPL junction and 9 μm below the OPL–ONL junction, thus including the OPL. **E.** B-scan showing the retinal layer segmentation provided by An-gioAnalytic software. From the inner retina to the outer retina: white line (ILM), yellow line (outer boundary of the nerve fiber layer), orange line (outer boundary of the IPL), red line (outer boundary of the INL), violet line (outer boundary of the OPL), and purple line (outer boundary of the retinal pigment epithelium).
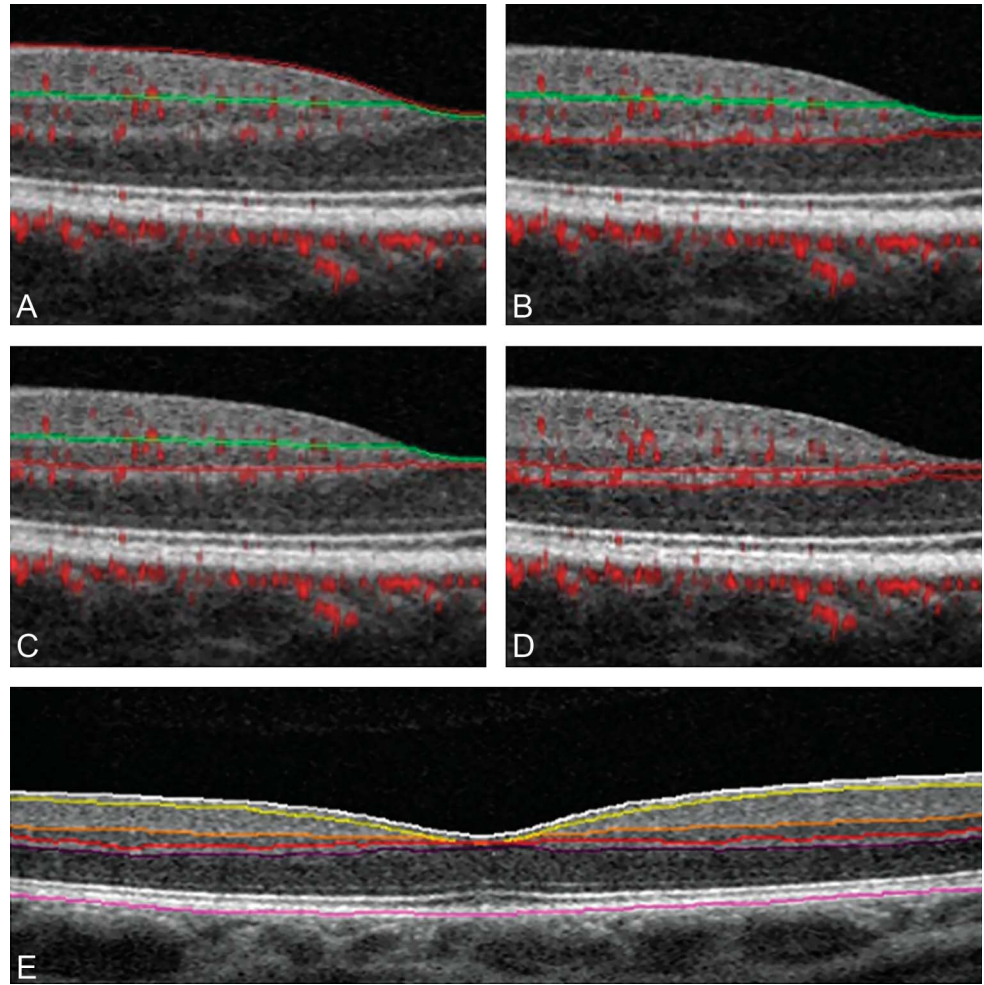
layers was evaluated. The SVP colocalizes with the ILM–IPL slab. The DVC colocalizes with the INL–OPL slab, thus including the INL and OPL layers. It should be noted that the segmentation used to generate capillary plexus images is not exactly the same that of the retinal layers on structural OCT. The capillary plexus projections are slightly offset compared with the corresponding retinal layers on structural OCT.[20]

Statistical Analysis

Continuous variables (VD and retinal thickness) are presented as mean and SD. Comparisons between continuous variable distributions were made using the nonparametric Wilcoxon Mann–Whitney and Kruskal–Wallis tests. The linear association between continuous variables was assessed by computing the Pearson's correlation coefficients with 95% confidence intervals calculated using the Fisher's z transformation or a linear regression model.[21] To account for intra-individual correlation, linear mixed-effect models for all eyes were fitted to evaluate the association between VD and retinal thickness measurements and age, by controlling for sex and image quality.[22]

Results

Vessel Density and Foveal Avascular Zone Data

Vessel density data are reported in Tables 2 and 3. Overall, the mean VD values (whole image and parafoveal areas, respectively, in %) within the vascular plexuses were 47.8 ± 2.8 and 50.5 ± 2.8 in the SVP, 52.7 ± 3.3 and 54.2 ± 3.2 in the DVC, 45.4 ± 4.2 and 46.9 ± 4.2 in the ICP, and 31.6 ± 4.4 and 32.7 ± 4.3 in the DCP. The DVC had the highest VD compared with other layers ($P < 0.001$), values being 4.9% and 3.8% higher than those found in the SVP within the whole and parafoveal areas, respectively. The DCP, the outer component of the DVC, had the lowest VD with a value
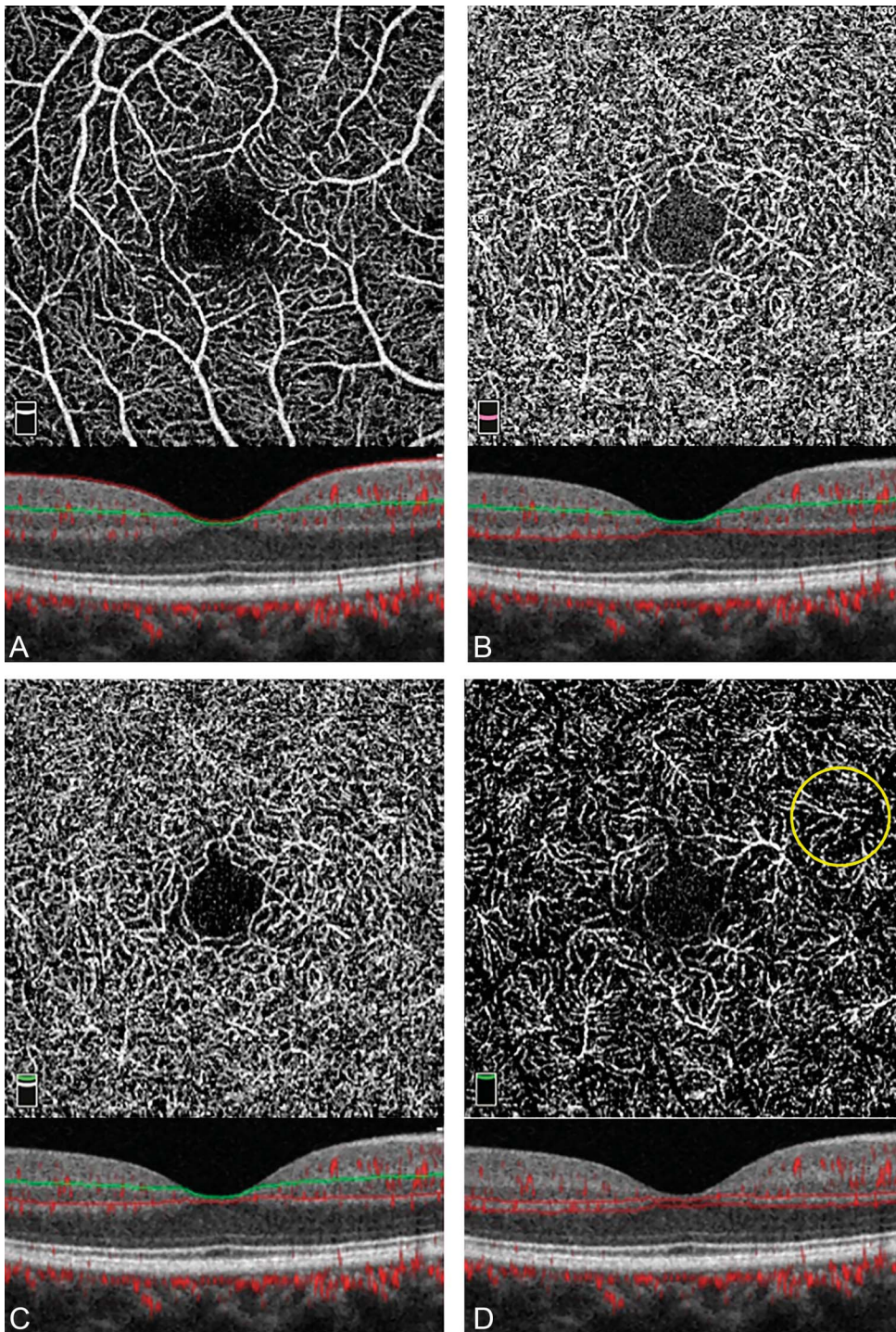
Fig. 2. Optical coherence tomography angiograms of retinal vascular plexuses. En face OCTA angiograms of four retinal vascular plexuses and corresponding OCT B-scans showing segmentation boundaries. **A.** Superficial vascular plexus. **B.** Deep vascular complex. **C.** Intermediate capillary plexus. **D.** Deep capillary plexus. The yellow circle indicates a capillary unit draining centrally.

accounting for about 2/3 of the ICP value (Figure 4). Note that we referred to as DCP the outer part of the DVC, a customized slab that isolates this monoplanar plexus of deep capillaries lying in the OPL.[15]

In the SVP, the overall VD was significantly higher in the superior (51.4 ± 3.3) and inferior (51.8 ± 3.1) sectors compared with the nasal (49.9 ± 2.7) and temporal (48.9 ± 3.0) sectors ($P < 0.001$)

(Table 3). Moreover, the SVP VD in the nasal sector was significantly greater than that in the temporal sector ($P = 0.003$). Conversely, no VD differences among sectors were observed in the DVC, ICP, and DCP.

Overall mean values for the FAZ, FAZ acircularity index, and FD-300 area were, respectively, 0.25 ± 0.11 mm^2, 1.14 ± 0.05, and 50.8 ± 3.4%.

Fig. 3. Optical coherence tomography angiography VD maps. **A.** Optical coherence tomography angiography map showing the contour (inner yellow ring) of the FAZ and a 300-μm wide area (limited by the outer yellow ring) where the flow density (FD-300) was calculated. **B.** Optical coherence tomography angiography map subdivision. An inner 1-mm diameter ring is centered on the fovea. The parafoveal area is included between the inner ring and the outer 3-mm diameter ring. Radial lines define parafoveal sectors (temporal, superior, nasal, and inferior) where the sectorial VD is measured. The whole VD is calculated in the totality of the 3 × 3-mm area. **C–E.** En face OCTA angiograms with color-coded VD (color bar: warmer colors representing the higher VD) of the four retinal vascular plexuses: SVP (**C**), DVC (**D**), ICP (**E**), and DCP (**F**). The DVC is the combination of the ICP and the DCP.
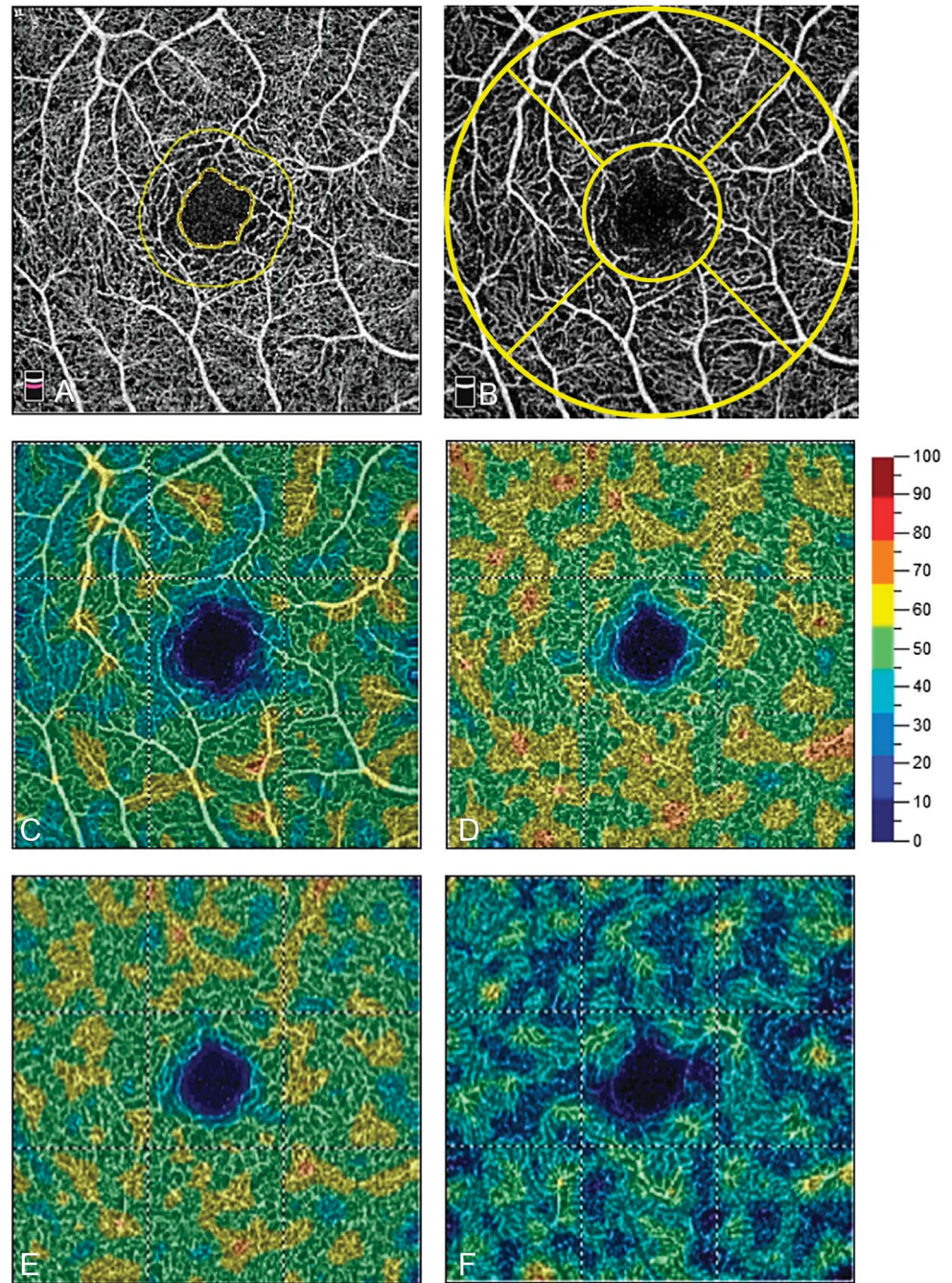
Vessel Density and Foveal Avascular Zone/FD-300 Variations According to Age, Sex, and Image Quality

Vessel density variations with age. Vessel density significantly decreased with age in all plexuses and all sectors of the macula (all $P < 0.01$, Figure 5). The mean VD decrease per year (%) was 0.064 in the SVP, 0.086 in the DVC, 0.055 in the ICP, and 0.076 in the DCP (values for the whole area). Vessel density values of all capillary plexuses according to age and sectors of the macula are provided in Table 3.

Vessel density variations with sex. No difference according to sex was found for the SVP VD, while in the DVC, ICP, and DCP, a significant difference was observed within the parafoveal area, women having a greater VD (%) (1.39, 1.54, and 1.31, $P = 0.006$, 0.003, and 0.032, respectively).

Vessel density variations with image quality. Although the eyes included in this study had a good

Table 2. Retinal VD, Retinal Thickness, and FAZ Parameters Within the Whole and Parafoveal Area

	Whole	Parafovea
VD (%)		
SVP	47.75 ± 2.83	50.49 ± 2.82
DVC	52.65 ± 3.30	54.24 ± 3.18
ICP	45.44 ± 4.16	46.91 ± 4.18
DCP	31.61 ± 4.36	32.68 ± 4.31
Thickness (μm)		
ILM–RPE	319.84 ± 12.42	329.99 ± 13.02
ILM–IPL	107.77 ± 7.62	113.43 ± 8.13
GCL–IPL	83.28 ± 6.19	90.79 ± 6.92
INL–OPL	65.66 ± 3.54	68.88 ± 3.94
INL	38.86 ± 2.39	41.58 ± 2.64
FAZ parameters		
FAZ area (mm^2)	0.25 ± 0.11	
FAZ perimeter (mm)	1.97 ± 0.43	
Acircularity Index	1.14 ± 0.05	
FD-300 area (%)	50.76 ± 3.43	

Data are provided as mean ± SD. Whole refers to the totality of the 3 × 3-mm OCTA area. Parafovea refers to the 3-mm diameter area excluding the central 1-mm diameter (foveal area).

Acircularity index refers to the ratio between the measured perimeter and the perimeter of the same size circular area. FD-300 area refers to the VD within a 300-μm wide area around the FAZ margin, calculated on a slab including both the SVP and the DVC.

RPE, retinal pigment epithelium.

SSI, i.e., greater than 70, the VD was still significantly related to SSI values. For every single unit increase of the SSI, the percentage of VD increased by 0.10% in the SVP, 0.14% in the DVC, 0.39% in the ICP, and 0.35% in the DCP (whole area, all $P < 0.05$). For example, for a VD of 50% in the SVP, the predicted effect of a change in the SSI of 5 points, accounting for age, sex, and QI, was expected to increase the VD to 50.5% (0.10%; 95% confidence interval: 0.03–0.17, $P = 0.003$). Conversely, the effect of the QI on VD, accounting for age, sex, and SSI, was smaller in magnitude and not statistically significant (0.03%; 95% confidence interval: −0.48 to 0.54, $P = 0.913$, SVP whole area).

Foveal avascular zone parameters and FD-300. The FAZ area and perimeter significantly and positively correlated with subject age. The increase in FAZ area per year of age was of 0.003 mm^2 ($P < 0.001$). Moreover, the FAZ area was significantly larger in women (0.057 mm^2, $P = 0.006$). Quality parameters were not related to the FAZ area and perimeter. The acircularity index and FD-300 area were not significantly related to subject characteristics or QI parameters.

Retinal Layer Thickness Data

Thickness data based on retinal slabs within the different areas, according to age, are provided in

Supplemental Digital Content 2 (see **Table 4**, http://links.lww.com/IAE/A946).

Retinal thickness sectorial analysis. The retinal thickness sectorial analysis revealed a distribution parallel to that of VD: the inner retinal thickness (ILM to IPL) was greater in the superior (116.6 ± 8.6 μm) and inferior (117.2 ± 8.5 μm) quadrants, followed by the nasal (113.9 ± 8.9 μm) and temporal (106.0 ± 8.0 μm) quadrants (all $P < 0.01$). The thickness of the deeper slabs did not differ according to the examined parafoveal quadrant.

Slab thickness variation with age and sex. A statistically significant reduction in ILM–IPL and GCL–IPL thickness with age was observed. Both the ILM–IPL and the GCL–IPL significantly decreased by 0.12 μm per year of age in the whole and parafoveal areas ($P < 0.05$). The total retinal thickness and the INL–OPL, as well as the INL alone, did not change according to subject age. The total retinal thickness was significantly greater in men than in women, with differences of 9 and 9.7 μm in the whole and parafoveal areas, respectively ($P < 0.001$). This trend was also found within the different retinal slabs (all $P < 0.05$).

Correlation Between Vessel Density and Retinal Thickness

The SVP VD and the ILM–IPL thickness both tended to decrease with age with a moderate positive correlation (0.56). Conversely, although the DVC VD also decreased with age, the thickness of the corresponding slabs (INL–OPL) did not significantly change, so that no correlation was found between these parameters.

Discussion

Through the use of a commercially available upgraded version of the amplitude decorrelation software of the Optovue device including the new 3D PAR algorithm (AngioVue, Phase 7 AngioAnalytic software), we were able to identify 3 distinct capillary layers in the macula: the SVP, the ICP, and the DCP in 148 healthy eyes of 84 subjects aged from 22 to 76 years. The PAR algorithm removes most of the flow projections from the SVP while preserving the density and the continuity of the ICP and the DCP.[12] It enables a clearer visualization and a more reliable VD calculation within each capillary plexus, in particular in the DCP, compared to previous software without PAR.

Clinically, OCTA begins to be used to quantify and assess the severity of microvascular changes in several

Table 3. Vessel Density Values (%) Within Four Plexuses According to Age and Image Sector

	Whole	Fovea	Parafovea	S Hemi	I Hemi	Temporal	Superior	Nasal	Inferior
SVP									
Overall	47.8 ± 2.8	21.3 ± 6.0	50.5 ± 2.8	50.3 ± 2.9	50.7 ± 2.9	48.9 ± 3.0	51.4 ± 3.3	49.9 ± 2.7	51.8 ± 3.1
22–26 y	48.9 ± 2.3	24.0 ± 5.2	51.4 ± 2.3	51.3 ± 2.4	51.6 ± 2.4	49.7 ± 2.6	52.5 ± 2.7	50.9 ± 2.0	52.6 ± 2.7
27–31 y	48.2 ± 2.2	23.5 ± 4.3	50.8 ± 2.4	50.7 ± 2.5	51.0 ± 2.5	49.4 ± 2.4	51.5 ± 3.1	50.4 ± 2.2	52.1 ± 2.8
32–39 y	47.8 ± 3.5	20.8 ± 7.3	50.8 ± 3.4	50.6 ± 3.4	51.0 ± 3.4	49.1 ± 3.6	51.5 ± 3.7	50.6 ± 3.1	51.9 ± 3.6
40–57 y	47.9 ± 2.4	19.9 ± 6.0	50.5 ± 2.5	50.3 ± 2.4	50.7 ± 2.7	48.7 ± 2.5	51.6 ± 2.8	49.5 ± 2.6	52.1 ± 2.9
>58 y	44.6 ± 2.5	15.5 ± 3.7	47.8 ± 3.0	47.6 ± 3.3	48.0 ± 2.9	46.5 ± 3.4	48.4 ± 3.9	47.5 ± 3.0	48.9 ± 2.8
DVC									
Overall	52.7 ± 3.3	36.0 ± 7.0	54.2 ± 3.2	54.4 ± 3.2	54.1 ± 3.2	54.4 ± 3.0	54.3 ± 3.6	54.5 ± 3.2	53.9 ± 3.6
22–26 y	53.7 ± 3.5	38.7 ± 5.3	55.3 ± 3.4	55.4 ± 3.5	55.2 ± 3.4	55.3 ± 3.4	55.4 ± 3.9	55.6 ± 3.0	54.9 ± 3.8
27–31 y	53.7 ± 2.8	40.0 ± 4.4	55.1 ± 2.6	55.2 ± 2.5	55.0 ± 2.9	55.4 ± 2.4	54.8 ± 2.9	55.5 ± 2.6	54.6 ± 3.6
32–39 y	53.9 ± 2.7	36.4 ± 6.5	55.5 ± 2.6	55.7 ± 2.6	52.2 ± 2.8	55.6 ± 2.6	55.8 ± 2.8	55.3 ± 2.8	55.2 ± 3.1
40–57 y	50.9 ± 2.9	32.0 ± 8.0	52.7 ± 2.8	52.9 ± 3.0	52.6 ± 2.8	52.9 ± 2.5	52.8 ± 3.6	53.0 ± 2.7	52.3 ± 3.3
>58 y	50.6 ± 3.0	31.7 ± 6.1	52.3 ± 3.2	52.3 ± 3.3	52.3 ± 3.2	52.5 ± 2.3	52.1 ± 3.6	52.3 ± 3.7	52.3 ± 3.3
ICP									
Overall	45.4 ± 4.2	32.7 ± 6.4	46.9 ± 4.2	46.9 ± 4.2	47.0 ± 4.2	47.0 ± 4.1	46.6 ± 4.7	47.4 ± 3.9	46.7 ± 4.5
22–26 y	47.0 ± 4.4	35.5 ± 4.5	48.5 ± 4.4	48.4 ± 4.4	48.6 ± 4.4	48.5 ± 4.3	48.3 ± 5.0	49.0 ± 3.9	48.2 ± 4.7
27–31 y	45.6 ± 3.7	36.2 ± 4.2	46.7 ± 3.6	46.7 ± 3.6	46.7 ± 3.7	47.0 ± 3.4	46.2 ± 3.9	47.4 ± 3.4	46.4 ± 4.2
32–39 y	45.6 ± 3.0	33.3 ± 6.3	48.1 ± 2.9	48.2 ± 2.8	48.0 ± 3.1	48.2 ± 2.9	48.0 ± 2.9	48.5 ± 3.1	47.8 ± 3.5
40–57 y	44.7 ± 4.1	29.2 ± 6.9	46.4 ± 4.4	46.4 ± 4.4	46.4 ± 4.4	46.6 ± 4.1	46.1 ± 5.1	46.6 ± 4.0	46.2 ± 4.7
>58 y	42.3 ± 4.0	27.8 ± 4.9	43.9 ± 4.3	43.8 ± 4.4	44.1 ± 4.2	43.8 ± 4.2	43.4 ± 4.7	44.6 ± 4.3	44.1 ± 4.3
DCP									
Overall	31.6 ± 4.4	22.3 ± 5.8	32.7 ± 4.3	32.8 ± 4.4	32.5 ± 4.3	32.6 ± 4.3	32.9 ± 4.6	32.8 ± 4.3	32.4 ± 4.6
22–26 y	33.8 ± 4.3	25.5 ± 5.0	34.9 ± 4.2	35.0 ± 4.2	34.8 ± 4.3	34.7 ± 4.4	35.0 ± 4.5	35.2 ± 4.0	34.7 ± 4.5
27–31 y	31.3 ± 3.9	23.2 ± 4.9	32.2 ± 3.8	32.5 ± 4.0	31.9 ± 3.8	32.5 ± 3.9	32.4 ± 4.0	32.5 ± 3.9	31.6 ± 4.3
32–39 y	33.5 ± 3.4	23.8 ± 4.6	34.5 ± 3.3	34.6 ± 3.2	34.5 ± 3.4	34.4 ± 3.7	34.9 ± 3.3	34.3 ± 3.2	34.5 ± 3.7
40–57 y	30.3 ± 4.1	18.8 ± 6.0	31.5 ± 4.0	31.6 ± 4.1	31.3 ± 4.0	31.3 ± 3.8	31.6 ± 4.5	31.6 ± 4.1	31.3 ± 4.3
>58 y	28.6 ± 4.2	19.9 ± 5.3	29.5 ± 4.3	29.7 ± 4.6	29.4 ± 4.2	29.5 ± 4.4	29.8 ± 4.9	29.4 ± 4.2	29.5 ± 4.4

Values are provided as mean ± SD. Whole refers to the totality of the 3 × 3-mm OCTA area. Fovea refers to the central 1-mm diameter circular area. Parafovea refers to the 3-mm diameter circular area excluding the foveal area.

S and I Hemi, respectively, refer to the superior and inferior 180° wide sectors of the parafoveal area. Temporal, superior, nasal, and inferior refer to 90° wide sectors of the parafoveal area.

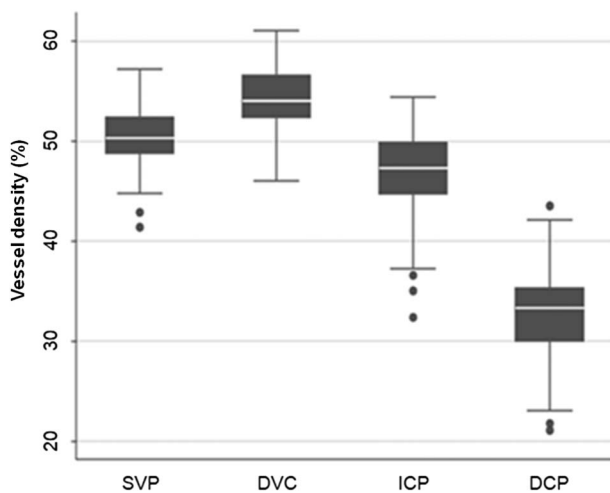I Hemi, inferior hemifield; S Hemi, superior hemifield.

Fig. 4. Vessel density of the retinal vascular plexuses in the overall population. Box-plots show parafoveal VD values within the SVP, DVC, ICP, and DCP. Vessel density (%) is represented on the y-axis. The VD is significantly different between each plexus (all $P < 0.001$), higher in the DVC, followed by the SVP, the ICP, and the DCP. Dots represent outside values. Upper and lower whiskers, respectively, represent the upper and lower adjacent values. Upper and lower box margins represent the 25th and 75th percentiles. The white line inside the box is the median value.

vascular diseases including diabetic retinopathy.[7–9,19,23] Numerous parameters have been tested such as FAZ metrics or VD or vessel length. It now seems necessary to have more reliable data on VD in healthy subjects using the most advanced software, in particular to accurately detect the DCP whose impairment seems to play a critical role in visual acuity decrease in diabetic maculopathy.[24]

Campbell et al[15] have first applied an algorithm similar to the one we used, to a small number of eyes of healthy subjects and have determined suitable parameters of segmentation to isolate each of these plexuses. They have divided the retinal circulation into two vascular complexes and four plexuses. The superficial vascular complex (SVC) consists of the SVP and the radial peripapillary capillary plexus. The DVC includes the ICP above the INL and the DCP below the INL. We used a comparable retinal segmentation and nomenclature in this study. We are aware that a small part of the radial peripapillary capillary plexus is present in the superior, inferior, and nasal parts of the 3 × 3-mm macular density map, but its presence is negligible, and we considered that the vessels
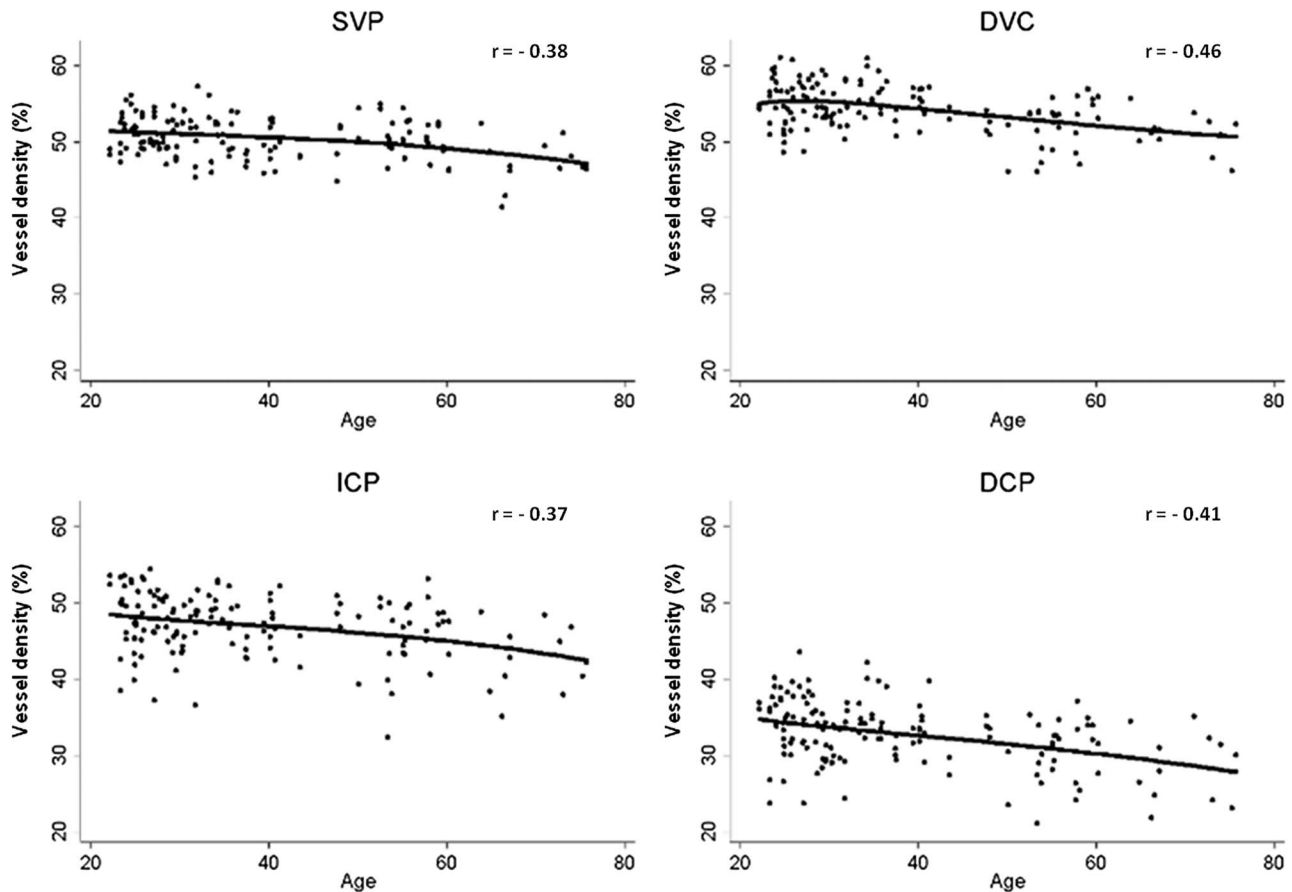
Fig. 5. Vessel density of retinal vascular plexuses in the overall population according to age. Scatter-plots with solid lines (representing the best fitting second-degree fractional polynomial) show parafoveal VD values within the SVP, DVC, ICP, and DCP according to subject age. The VD (%) is represented on the y-axis. Age (years) is represented on the x-axis. The VD is significantly decreased per year of age within each plexus (all $P < 0.001$). r = Pearson correlation coefficient.

comprised between the ILM and an inner portion of the IPL form the SVP. However, this may explain the small differences in ILM–IPL thickness and in SVP VD between the nasal and temporal parts of the 3 × 3-mm OCTA VD map (see **Figure 6, Supplemental Digital Content 1**, http://links.lww.com/IAE/A945). From a practical perspective, we considered that there were three capillary plexuses in the macular and parafoveal areas.

Of the three macular capillary plexuses, only one, the DCP, has been described as a single monoplanar capillary layer on OCTA and in histological studies,[3–5] while the ICP and the SVP have a multiplanar architecture.[5,25,26]

It is thus not surprising that we found that the VD was higher in the SVP and the ICP than in the DCP. To be able to compare our results with those reported in other publications that did not express their results in the same units, we used the ratio between VD values of each plexus. In our study, the ratio between the SVP and DCP densities in the parafoveal area was

1.55; by comparison, it was 2.15 in the study by Campbell et al,[15] who did not select the same surface of parafoveal area, and it was 1.65 in a histological study by Tan et al,[5] who used quantitative confocal imaging. However, the ratio was 0.95 in the OCTA study by Garrity et al[17] who used a wider slab to segment the DCP and probably incorporated some elements of the ICP. Regarding the ICP density, we found a SVP/ICP ratio of 1.07 compared with 1.27 for Campbell et al[15] and 0.89 for Garrity et al,[17] here again, this could be due to differences when segmenting the slab corresponding to the ICP.

The ICP and the SVP are denser and have a multiplanar organization.[3,5,27] Their projection on one plane probably does not allow for measuring the actual density of these plexuses.[26] We are also aware that OCTA, because of the limitation of its lateral resolution, overestimates the size of capillaries, which in fact are thinner and much more spaced than shown on OCTA maps. This has been demonstrated in several histological studies,[3,5,6] and in vivo in humans using Adaptive

Optics-OCTA.[28] For instance, Yu et al[3] have studied a microperfused human retina by confocal microscopy and reported that the superficial capillaries cover about 30% of the examined field while the deep capillaries cover about 17%, whereas in this study, the values were, respectively, of 50% and 30% to 35%. However, the ratio between the VD of each capillary plexus measured on OCTA with PAR is close to the results reported in histological studies.[3,5,27]

The laminated organization of retinal capillaries is supposed to serve to the metabolic support of the different retinal layers. Although the capillaries of the SVP are immersed in the GCL, the INL, which also contains the nuclei of Müller cells, is devoid of capillaries and only framed by the ICP and the DCP located in the plexiform layers. The reasons why these two plexuses have different organizations are unknown. The multiplanar ICP is located in the IPL containing synapses between bipolar and ganglion cells as well as amacrine cells.[5,29]The DCP is located in the OPL, which is thinner than the IPL and composed of synapses of photoreceptors and bipolar cells, and horizontal cells.[5] This area is also at the border of the oxygen diffusion from the choroid.[30] Because of the low partial pressure of oxygen level in the ONL, it is likely that the oxygen coming from the choroid has been completely consumed by the photoreceptors, mainly cones, and that the DCP is needed for supplying both bipolar cells and the synaptic machinery of the OPL and Henle fibers.[30]

Although the functional organization of the three capillary layers is not the subject of this article and remains controversial, it is likely that, based on the density we measured, the ICP and the DCP form a functional complex (DVC), with a different pattern compared with the SVP,[4,16,31] and aimed to supply the metabolic needs of the INL and its plexiform layers, including cells such as amacrine and horizontal cells, and Müller cells.

We found that the VD decreased with age, to a greater extent in the DCP than in the SVP, in line with the results by Garrity et al[17]. This difference in density decrease with age between the DCP and the SVP has not been shown in studies that did not use PAR software.[32,33] The influence of age seems to be greater at the DCP, which could be more sensitive to pathological conditions.

We also found that the FAZ area and perimeter significantly and positively correlated with subject age in our study as already observed by others.[32] In addition, we found that the FAZ was larger in women, which could be due to a thinner fovea.[34]

In future studies on retinal vascular diseases, several parameters including the VD in the three capillary plexuses, and FAZ parameters should be measured.[19] They could evolve differently with age and disease and have different impacts on visual function.

Finally, we showed that the VD varied with image quality. The decrease in SSI has already been incriminated to explain, at least partially, the reduction in VD in case of macular edema.[23,35] This study conducted in healthy eyes confirms that the SSI, but not the QI, influences VD values. We encourage the use of both quality parameters for further analysis. This study including a large sample of healthy subjects showed that the new currently available software of Optovue provides valuable data of VD in the SVP and the DVC, as well as in the ICP and DCP sublayers.

Our study has several strengths. We studied a large cohort of healthy eyes of subjects with a wide range of age. Unlike other studies,[15,17] we used the currently available device software to calculate the VD. We took full advantage of the new 3D PAR algorithm, a software that is currently available, and of an adjusted segmentation to isolate 3 separate capillary beds, the SVP, the ICP, and the DCP. We showed a reliable capillary density measurement in the DCP in a large number of eyes. The capillary density of the DVC, including both the ICP and the DCP, was also shown. Moreover, we showed the sensitivity of VD measurement at the SSI level, and this should be taken into account, especially when studying older populations that are more likely to develop lens opacity.

However, we recognize that our study has some limitations. The study population had a mean age of 41.3 years, with a median age of 35.7 years and 18% of subjects were 58 years or older, which could be a disadvantage for studying retinal vasculopathies in the elderly. However, measuring retinal VD is mainly useful in the preclinical or early stage of vascular retinal diseases.[19] For this purpose, this cohort of healthy subjects could be used as a comparator for diseases appearing in young or middle-aged patients such as Type 1 diabetic retinopathy.[24] Moreover, it shows that age-related VD decrease should be taken into account when studying older cohorts of patients. Despite the improved speed and quality of OCTA image acquisition, we had to exclude 34 healthy eyes (18.7%) with normal vision from the initial cohort because of obvious image artifacts. We did not take into account the axial length but, because of the small refractive error of the included eyes, it should not change the VD. We are aware that the adequacy between the capillary plexus segmentation and the retinal tissue segmentation may not be perfect.[20] Indeed, the principle of OCTA is to offset the projection of flow a bit deeper than the retinal layers in which the vessels really are.[20] However, the correlation between

the VD and the retinal layer thickness as segmented on structural OCT should be investigated in a future study. Finally, although we applied the manufacturer parameters to delineate the boundaries of the SVP and the DVC, we used an additional customized segmentation to delineate the boundaries of the ICP and the DCP for which no consensus has yet been reached. However, this segmentation fits at least partially with the most recent data from histological studies.

In conclusion, in this study, we used an upgraded OCTA software enhanced with PAR to measure the macular capillary density, not only in the SVP and the DVC, but also in the two sublayers of the DVC, i.e., the ICP and the DCP. Foveal avascular zone metrics and retinal layer thickness were also recorded. Vessel density measurements were made in the whole 3 × 3-mm area of the VD map and the various sectors of the parafovea. In healthy eyes, the capillary density of the DCP, a single monoplanar capillary plexus, is much lower than that of the SVP and the ICP. Capillary density decreases with age in all plexuses, but to a greater extent in the DCP, while the FAZ increases in size. The vascular density is sensitive to the SSI even in normal eyes. The study of these parameters obtained in 148 healthy eyes of subjects belonging to different age groups provides a method to compare macular density between groups with retinal vascular diseases and control groups.

Key words: capillary density, deep capillary plexus, intermediate capillary plexus, OCTA, optical coherence tomography angiography, retina, retinal capillaries, retinal capillary plexus, retinal vessel density.

Acknowledgments

References

1. Jia Y, Tan O, Tokayer J, et al. Split-spectrum amplitude-decorrelation angiography with optical coherence tomography. Opt Express 2012;20:4710–4725.
2. Spaide RF, Klancnik JM Jr, Cooney MJ. Retinal vascular layers imaged by fluorescein angiography and optical coherence tomography angiography. JAMA Ophthalmol 2015;133:45–50.
3. Yu PK, Mammo Z, Balaratnasingam C, Yu DY. Quantitative study of the macular microvasculature in human donor eyes. Invest Ophthalmol Vis Sci 2018;59:108–116.
4. Fouquet S, Vacca O, Sennlaub F, Paques M. The 3D retinal capillary circulation in pigs reveals a predominant serial organization. Invest Ophthalmol Vis Sci 2017;58:5754–5763.
5. Tan PE, Yu PK, Balaratnasingam C, et al. Quantitative confocal imaging of the retinal microvasculature in the human retina. Invest Ophthalmol Vis Sci 2012;53:5728–5736.
6. Snodderly DM, Weinhaus RS, Choi JC. Neural-vascular relationships in central retina of macaque monkeys (Macaca fascicularis). J Neurosci 1992;12:1169–1193.
7. Agemy SA, Scripsema NK, Shah CM, et al. Retinal vascular perfusion density mapping using optical coherence tomography angiography in normals and diabetic retinopathy patients. Retina 2015;35:2353–2363.
8. Coscas F, Glacet-Bernard A, Miere A, et al. Optical coherence tomography angiography in retinal vein occlusion: evaluation of superficial and deep capillary plexa. Am J Ophthalmol 2016;161:160–171.e161–162.
9. Minvielle W, Caillaux V, Cohen SY, et al. Macular microangiopathy in sickle cell disease using optical coherence tomography angiography. Am J Ophthalmol 2015;164:137–144 e131.
10. Philippakis E, Dupas B, Bonnin P, et al. Optical coherence tomography angiography shows deep capillary plexus hypoperfusion in incomplete central retinal artery occlusion. Retin Cases Brief Rep 2015;9:333–338.
11. Spaide RF, Fujimoto JG, Waheed NK. Image artifacts in optical coherence tomography angiography. Retina 2015;35:2163–2180.
12. Hwang TS, Zhang M, Bhavsar K, et al. Visualization of 3 distinct retinal plexuses by projection-resolved optical coherence tomography angiography in diabetic retinopathy. JAMA Ophthalmol 2016;134:1411–1419.
13. Zhang A, Zhang Q, Chen CL, Wang RK. Methods and algorithms for optical coherence tomography-based angiography: a review and comparison. J Biomed Opt 2015;20:100901.
14. Camino A, Zhang M, Gao SS, et al. Evaluation of artifact reduction in optical coherence tomography angiography with real-time tracking and motion correction technology. Biomed Opt Express 2016;7:3905–3915.
15. Campbell JP, Zhang M, Hwang TS, et al. Detailed vascular anatomy of the human retina by projection-resolved optical coherence tomography angiography. Sci Rep 2017;7:42201.
16. Bonnin S, Mane V, Couturier A, et al. New insight into the macular deep vascular plexus imaged by optical coherence tomography angiography. Retina 2015;35:2347–2352.
17. Garrity ST, Iafe NA, Phasukkijwatana N, et al. Quantitative analysis of three distinct retinal capillary plexuses in healthy eyes using optical coherence tomography angiography. Invest Ophthalmol Vis Sci 2017;58:5548–5555.
18. Mo S, Krawitz B, Efstathiadis E, et al. Imaging foveal microvasculature: optical coherence tomography angiography versus adaptive optics scanning light ophthalmoscope fluorescein angiography. Invest Ophthalmol Vis Sci 2016;57:OCT130–140.
19. Alibhai AY, Moult EM, Shahzad R, et al. Quantifying microvascular changes using OCT angiography in diabetic eyes without clinical evidence of retinopathy. Ophthalmol Retina 2017;2:418–427.
20. Spaide RF, Fujimoto JG, Waheed NK, et al. Optical coherence tomography angiography. Prog Retin Eye Res 2018;64:1–55.
21. Gleason JR. Inference about correlations using the Fisher z-transform. Stata Tech Bull 1996;6:18.
22. Graubard BI, Korn EL. Modelling the sampling design in the analysis of health surveys. Stat Methods Med Res 1996;5:13–18.
23. Samara WA, Shahlaee A, Adam MK, et al. Quantification of diabetic macular ischemia using optical coherence tomography

angiography and its relationship with visual acuity. Ophthalmology 2017;124:235–244.

24. Dupas B, Minvielle W, Bonnin S, et al. Association between vessel density and visual acuity in patients with diabetic retinopathy and poorly controlled Type 1 diabetes. JAMA Ophthalmol 2018;136:721–728.

25. Yu J, Gu R, Zong Y, et al. Relationship between retinal perfusion and retinal thickness in healthy subjects: an optical coherence tomography angiography study. Invest Ophthalmol Vis Sci 2016;57:OCT204–210.

26. Balaratnasingam C, An D, Sakurada Y, et al. Comparisons between histology and optical coherence tomography angiography of the periarterial capillary-free zone. Am J Ophthalmol 2018;189:55–64.

27. Chan G, Balaratnasingam C, et al. Quantitative morphometry of perifoveal capillary networks in the human retina. Invest Ophthalmol Vis Sci 2012;53:5502–5514.

28. Salas M, Augustin M, Ginner L, et al. Visualization of microcapillaries using optical coherence tomography angiography with and without adaptive optics. Biomed Opt Express 2017; 8:207–222.

29. Park JJ, Soetikno BT, Fawzi AA. Characterization of the middle capillary plexus using optical coherence tomography angiography in healthy and diabetic eyes. Retina 2016;36: 2039–2050.

30. Linsenmeier RA, Zhang HF. Retinal oxygen: from animals to humans. Prog Retin Eye Res 2017;58:115–151.

31. Chang MY, Phasukkijwatana N, Garrity S, et al. Foveal and peripapillary vascular decrement in migraine with aura demonstrated by optical coherence tomography angiography. Invest Ophthalmol Vis Sci 2017;58:5477–5484.

32. Iafe NA, Phasukkijwatana N, Chen X, Sarraf D. Retinal capillary density and foveal avascular zone area are age-dependent: quantitative analysis using optical coherence tomography angiography. Invest Ophthalmol Vis Sci 2016; 57:5780–5787.

33. Coscas F, Sellam A, Glacet-Bernard A, et al. Normative data for vascular density in superficial and deep capillary plexuses of healthy adults assessed by optical coherence tomography angiography. Invest Ophthalmol Vis Sci 2016;57:OCT211–223.

34. Tick S, Rossant F, Ghorbel I, et al. Foveal shape and structure in a normal population. Invest Ophthalmol Vis Sci 2011;52: 5105–5110.

35. Chetrit M, Bonnin S, Mane V, et al. Acute pseudophakic cystoid macular edema imaged by optical coherence tomography angiography. Retina 2018;38:2073–2080.